

# DNAzymes as Catalysts for L-Tyrosine and Amyloid $\beta$ Oxidation

Tony Köhler, Panagiotis A. Patsis, Dominik Hahn, André Ruland, Carolin Naas, Martin Müller, and Julian Thiele\*



Cite This: *ACS Omega* 2020, 5, 7059–7064



Read Online

ACCESS |



Metrics & More

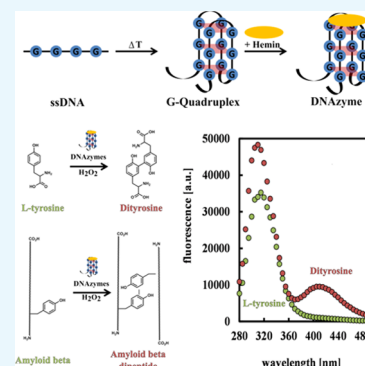


Article Recommendations



Supporting Information

**ABSTRACT:** Single-stranded deoxyribonucleic acids have an enormous potential for catalysis by applying tailored sequences of nucleotides for individual reaction conditions and substrates. If such a sequence is guanine-rich, it may arrange into a three-dimensional structure called G-quadruplex and give rise to a catalytically active DNA molecule, a DNAzyme, upon addition of hemin. Here, we present a DNAzyme-mediated reaction, which is the oxidation of L-tyrosine toward dityrosine by hydrogen peroxide. With an optimal stoichiometry between DNA and hemin of 1:10, we report an activity of  $101.2 \pm 3.5 \mu\text{Units}$  ( $\mu\text{U}$ ) of the artificial DNAzyme Dz-00 compared to  $33.0 \pm 1.8 \mu\text{U}$  of free hemin. Exemplarily, DNAzymes may take part in neurodegeneration caused by amyloid beta ( $A\beta$ ) aggregation due to L-tyrosine oxidation. We show that the natural, human genome-derived DNAzyme In1-sp is able to oxidize  $A\beta$  peptides with a 4.6% higher yield and a 33.3% higher velocity of the reaction compared to free hemin. As the artificial DNAzyme Dz-00 is even able to catalyze  $A\beta$  peptide oxidation with a 64.2% higher yield and 337.1% higher velocity, an in-depth screening of human genome-derived DNAzymes may identify further candidates with similarly high catalytic activity in  $A\beta$  peptide oxidation.



## INTRODUCTION

Deoxyribonucleic acid (DNA) codes the genetic information of proteins and determines their expression, for example, by different promoter sequences.<sup>1</sup> Beyond this basic function of life, DNA has been utilized in a vast number of applications, for example, in sensors,<sup>2</sup> for hydrogel formation,<sup>3,4</sup> or as a hemin-assembled catalyst.<sup>5–7</sup> In the latter case, the catalytic activity of DNAzymes was first described by Breaker in 1994.<sup>8</sup> Several techniques have been developed to investigate the spatial arrangement of single-stranded deoxyribonucleic acids (ssDNA) that form G-quadruplexes *in vitro* and *in vivo* as well as their ability to assemble with porphyrin-based guest molecules such as hemin or *N*-methyl mesoporphyrin IX into catalytically active DNAzymes.<sup>6,9,10</sup> Besides classical analytical tools such as immunofluorescence, bioinformatic tools have already been developed identifying approximately 300,000 sequences with the ability to form G-quadruplexes in the human genome.<sup>9,11,12</sup> There are numerous peroxidase-like reactions that DNAzymes have been applied to.<sup>3–6</sup> Along these lines, the oxidation of the amino acid L-tyrosine and its derivatives is well known to occur in a number of biological processes<sup>13–15</sup> and has been studied with horse radish peroxidase<sup>16</sup> as well as active DNAzymes.<sup>17–21</sup> For instance, L-tyrosine oxidation is one of the targets discussed in the development of neurodegenerative diseases such as Alzheimer's disease (AD) or Parkinson's disease.<sup>14,22</sup> In the former case, L-tyrosine in the peptide sequence of amyloid beta ( $A\beta$ ) 1–40 is oxidized to dityrosine, triggering peptide aggregation, which causes fibrillation and plaque formation in

the brain.<sup>13,15,23</sup> The molecular mechanism of L-tyrosine oxidation by  $A\beta$  itself is still not fully clarified.<sup>24</sup> Nevertheless, a correlation between oxidative stress and peroxidase activity has already been shown.<sup>15</sup> Here, we investigate different DNAzymes, natural as well as artificial sequences, as catalysts for the oxidation of L-tyrosine. We use In1-sp, a segment of the insulin-linked polymorphic region upstream of the insulin gene in the human genome, as a natural DNAzyme.<sup>2</sup> As an artificial DNAzyme, we use Dz-00 as a well-studied sequence.<sup>5,25</sup> Additionally, we employ these DNAzymes for the oxidation of  $A\beta$  1–40 to elucidate their catalytic efficiency as well as the potential contribution of DNAzymes in the development of neurodegenerative diseases.

## RESULTS

**DNAzyme Formation.** To form a catalytically active DNAzyme, ssDNA was heated up to 85 °C and slowly cooled down to room temperature for 30 min to form a G-quadruplex. The formation of the G-quadruplex was investigated by CD spectroscopy (Figure S1). Afterward, the G-quadruplex was mixed with hemin, and the absorption spectra were recorded

Received: August 16, 2019

Accepted: March 5, 2020

Published: March 27, 2020



(Figure 1). Here, a significant increase in absorption occurred compared to free hemin solution, indicating the formation of a

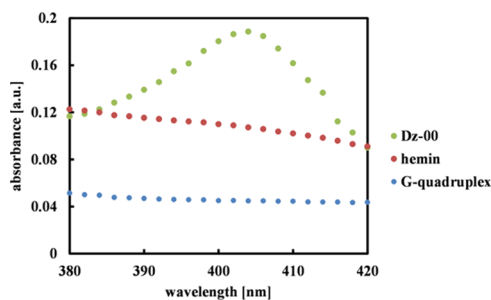


**Figure 1.** Absorption spectra after the formation of catalytically active Dz-00 (green) as well as hemin (red) and G-quadruplex (blue) for comparison.

functional DNAzyme by the addition of hemin. The G-quadruplex solution does not show prominent peaks in the absorption spectra.

The addition of hemin leads to the formation of the characteristic Soret band at 404 nm, as shown in Figure 1. This formation is determined by an equilibrium between assembly and disassembly of hemin and G-quadruplex (Figure S2). After the equilibrium between hemin and G-quadruplex was reached, which takes 4–9 min with decreasing concentration of hemin (Figure S2), the absorption spectra of hemin and DNAzymes were investigated with a maximum of absorption at 404 nm for Dz-00.

**L-Tyrosine Oxidation Catalyzed by Hemin.** To investigate the oxidation of L-tyrosine with hydrogen peroxide catalyzed by free hemin, the fluorescence emission spectra of the samples were measured from 280 to 500 nm in 5 nm increments. Initially, a dominant peak at 305 nm was monitored. This peak was identified as a characteristic peak for L-tyrosine in the reaction. However, we expected that the product of this reaction, dityrosine, also should have a fluorescence peak in that region. Immediately after adding hydrogen peroxide ( $\text{H}_2\text{O}_2$ ), we also observed a change in emission spectra by an increase in a broad range from 380 to 470 nm with a maximum at 405 nm (Figure 2).

The increasing emission at 305 nm is unsuitable for determining the apparent oxidation product. The more specific emission at 405 nm allows for quantifying dityrosine formation via free hemin (Figures S3 and S4). Additionally, HPLC–MS

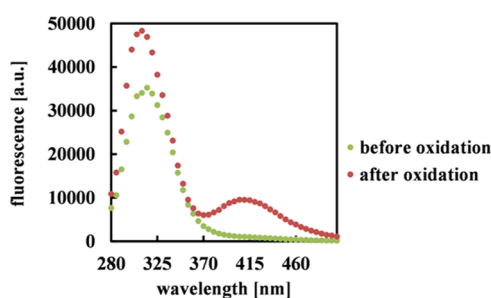


**Figure 2.** Fluorescence spectra of L-tyrosine (green) before and after oxidation to dityrosine (red). The fluorescence spectra showed a strong increase in fluorescence from 380 to 470 nm during L-tyrosine oxidation.

was performed to support the fluorescence measurements (Figures S5 and S6).

**L-Tyrosine Oxidation Catalyzed by DNAzymes.** To investigate the catalytic activity of the DNAzyme Dz-00, 250  $\mu\text{M}$  L-tyrosine and equimolar amounts of  $\text{H}_2\text{O}_2$  were added. Dityrosine formed immediately as measured by an increase of fluorescence monitored at 405 nm. We observed a significant increase in fluorescence when the reaction is catalyzed by Dz-00 compared to the oxidation of L-tyrosine with free hemin only (Figure 3).

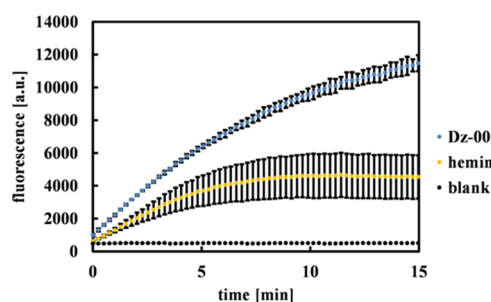


**Figure 3.** Time-dependent L-tyrosine oxidation by 100 nM free hemin (yellow) and 100 nM Dz-00 (blue). Dz-00 was supplemented by equimolar free hemin. The reaction contained 250  $\mu\text{M}$  L-tyrosine and was started by adding 250  $\mu\text{M}$   $\text{H}_2\text{O}_2$ . No reaction was observed, when Dz-00 was mixed with L-tyrosine in the absence of  $\text{H}_2\text{O}_2$  (black data points). Error bars indicate standard deviations of three independent measurements.

To further investigate the oxidation reaction of L-tyrosine, we varied the stoichiometry of hemin to G-quadruplex. The concentration of G-quadruplex was kept constant at 100 nM per reaction, whereas the hemin concentration was adjusted from equimolar up to 20-fold of the DNA concentration. The results show that whenever as-formed DNAzymes were used to catalyze the reaction, the activity was elevated compared to free hemin. A 10-fold excess of DNA was also investigated but did not alter the activity of the DNAzyme as the hemin was completely complexed by DNA with a stoichiometry of 1:1 already (Figure S7). The activities were determined in  $\mu\text{Units}$  ( $\mu\text{U}$ ) to elucidate the most efficient catalytic stoichiometry. A stoichiometry of 1:10 gave the highest activity with  $101.2 \pm 3.5$   $\mu\text{U}$  when catalyzed with Dz-00 (Figure 4). Interestingly, the free hemin at 1:10 stoichiometry showed a reduced activity

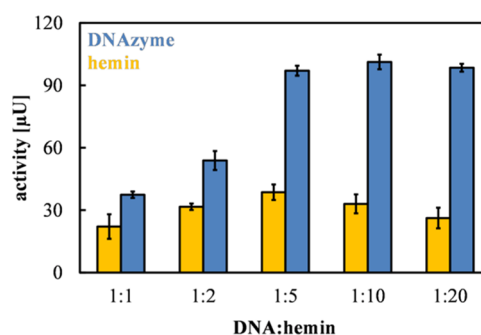


**Figure 4.** Stoichiometry test of Dz-00 (blue) and free hemin (yellow). Stoichiometries of 1:1, 1:2, 1:5, 1:10, and 1:20 of DNA (fixed to 100 nM) to hemin were tested to identify the ratio that gave the highest activity. The concentrations of L-tyrosine and  $\text{H}_2\text{O}_2$  used in the experiments were set to 250  $\mu\text{M}$ .

compared to the free hemin used at 1:5. Therefore, further experiments were performed at a stoichiometry of DNA to hemin with 1:10 ratio.

To investigate the influence of DNA sequence modifications on the catalytic activity of the corresponding DNAzyme, we tested if the addition of single nucleotides, proximal or distal to the sequences, would change their activity.

Therefore, Dz-11 to Dz-18 (Table 1) was applied to the *L*-tyrosine oxidation reaction and tested for their activity, again

**Table 1. Sequences of DNAzymes Investigated in This Study<sup>a</sup>**

Name	Sequence
In1-sp <sup>[2]</sup>	ACAGGGGTGTGGGGACAGGGGTGTGGGG
Dz-00 <sup>[25]</sup>	GGGTAGGGCGGGTTGGG
Dz-11 <sup>[5]</sup>	GGGTAGGGCGGGTTGGGA
Dz-12 <sup>[5]</sup>	GGGTAGGGCGGGTTGGGT
Dz-13 <sup>[5]</sup>	GGGTAGGGCGGGTTGGGG
Dz-14 <sup>[5]</sup>	GGGTAGGGCGGGTTGGGC
Dz-15 <sup>[5]</sup>	AGGGTAGGGCGGGTTGGG
Dz-16 <sup>[5]</sup>	TGGGTAGGGCGGGTTGGG
Dz-17 <sup>[5]</sup>	GGGGTAGGGCGGGTTGGG
Dz-18 <sup>[5]</sup>	CGGGTAGGGCGGGTTGGG

<sup>a</sup>Modifications of the reference Sequence Dz-00 are highlighted in red.

with a stoichiometry of 1:10. To compare the different sequences, the fold increase of fluorescence at 405 nm for DNAzymes over free hemin was calculated. We observed no significant differences in the activity of the chosen sequence changes of Dz-00 (Figure 5).

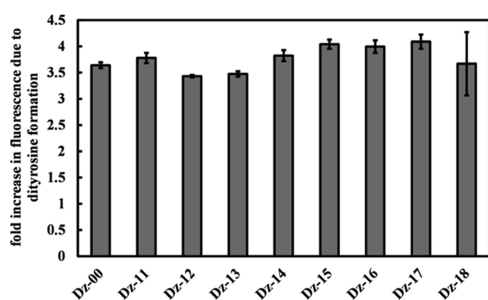


**Figure 5.** Influence on activity by modifying the sequence of Dz-00. The fluorescence fold increases of different sequences applied to the reaction are depicted.

**Oxidation of A $\beta$  by DNAzymes.** To link this peroxidase-like reaction to meaningful physiological processes, we applied the A $\beta$  peptide 1–40 with equimolar H<sub>2</sub>O<sub>2</sub> as reactants to Dz-00. We again observed an increase in fluorescence at 405 nm similar to the oxidation of *L*-tyrosine that is described above. Interestingly, when employing the DNA sequence In1-sp as a natural DNAzyme, we likewise detected oxidation of A $\beta$ . The reaction ran for about 35 min when catalyzed with In1-sp or hemin. However, we observed an increase of the slope by 33.3% and a yield of 4.6% by In1-sp compared to free hemin. Compared to that the DNA sequence Dz-00 showed a significantly higher increase in slope of 337.1%. We also

observed a significantly higher oxidation of the A $\beta$  peptide by Dz-00 by a 64.2% higher fluorescence (Figure 6).

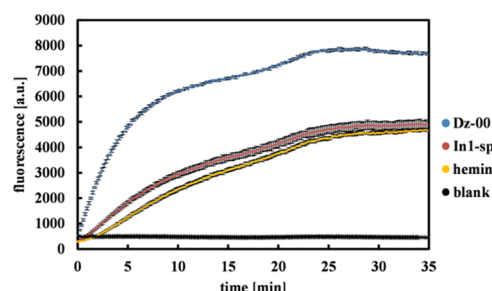


**Figure 6.** Oxidation of A $\beta$  1–40. Comparison of Dz-00 (blue), In1-sp (red), and free hemin (yellow) as well as a control (black). DNAzymes were supplemented with hemin by a molar stoichiometry of 1:10. The starting concentration of A $\beta$  and H<sub>2</sub>O<sub>2</sub> was 125  $\mu$ M.

### High-Performance Size Exclusion Chromatography Measurements of Oxidized A $\beta$ 1–40.

After reacting A $\beta$  1–40 with DNAzymes Dz-00 and In1-sp or with free hemin, samples were analyzed by high-performance size exclusion chromatography (HPSEC) and compared to reference samples of untreated A $\beta$  peptide. PBS buffer was used as the eluent. The samples were analyzed with a fluorescence detector, using an excitation wavelength of 250 nm and an emission wavelength of 305 and 405 nm. The retention time of A $\beta$  1–40 was 20.6 min (Figure 7A). The A $\beta$  1–40 dimer eluted

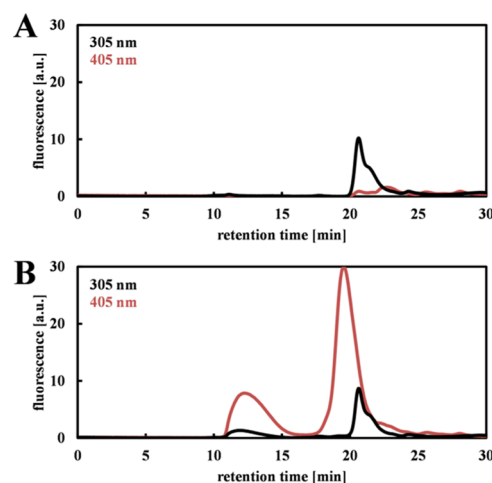


**Figure 7.** HPSEC chromatograms of nonoxidized A $\beta$  1–40 (A) and Dz-00-oxidized A $\beta$  1–40 (B). (A) Chromatogram indicates non-oxidized A $\beta$  in size exclusion chromatography excited at 250 nm and emission measured at 305 nm (black) and 405 nm (red), respectively. (B) Dz-00-oxidized A $\beta$  1–40 excited at 250 nm and emission measured at 305 nm (black) and 405 nm (red), respectively.

after 19.6 min (Figure 7B). To ensure that the A $\beta$  1–40 dimer was formed by the oxidation reaction, matrix-assisted laser desorption/ionization time-of-flight mass spectrometry (MALDI-TOF MS) was applied, and detected masses indicated A $\beta$  1–40 with 4345.5 and the A $\beta$  1–40 dimer with 8727.3 (Figure S9). The peak of the species eluting before A $\beta$  1–40 dimer at approximately 13 min belongs to an even bigger molecule expressing both emission wavelengths of 305 and 405 nm (Figure 7B). This peak was assigned to undefined aggregates of A $\beta$ <sup>15</sup> after oxidation.



## DISCUSSION

Here, we report the oxidation of L-tyrosine to dityrosine catalyzed by DNAzymes. For that, we investigated the model DNAzyme Dz-00.<sup>25</sup> Our results show that a molar ratio of 1:10 (DNA to hemin) gave the most active as-formed DNAzyme. While the activity of DNAzyme rose, the activity of free hemin decreased with increased concentrations of hemin.

The 3-fold increase of the activity of the DNAzymes compared to free hemin at molar ratios of 1:10 showed remarkable effects. The results of sequence modifications of Dz-00 did not favor any of the sequences over others in terms of catalytic activity of the corresponding DNAzyme. The sequences applied to L-tyrosine oxidation were chosen as reported from Li and co-workers.<sup>5</sup> We investigated if the intramolecular enhancement effect of the adjacent adenine at the 3' end of the sequences was an ubiquitous effect. Yet, none of the sequences tested from Dz-11 to Dz-18 showed a significant increase in fluorescence due to dityrosine formation compared to Dz-00 (Figure 5), suggesting that the reported enhancement effect could be utilized for the oxidation of 2,2'-azino-bis(3-ethylbenzothiazoline-6-sulponic acid), as shown by Li and co-workers,<sup>5</sup> but not for the oxidation of L-tyrosine, as the substrates differ rather significantly in their structure. The mechanism of the oxidation reaction was further investigated by electron paramagnetic resonance spectroscopy (Figure S11A). We demonstrated the formation of hydroxyl radicals when applying H<sub>2</sub>O<sub>2</sub> to Dz-00. The hydroxyl radicals further oxidize L-tyrosine to form tyrosyl radicals which react by coupling to form dityrosine. A proposed mechanism was presented in Figure S11B.

L-Tyrosine oxidation based on the DNA sequence for Dz-00 was then applied to oxidize the A $\beta$  1–40 peptide, which is known for being involved in the development of neurodegenerative diseases such as AD.<sup>22,26</sup> The oxidation of the A $\beta$  1–40 peptide is known to be catalyzed by metal ions such as copper, zinc, and iron or by free hemin when complexed with the A $\beta$  1–40 peptide.<sup>14,27,28</sup> Here, we report an additional mechanism of A $\beta$  1–40 peptide oxidation by DNAzymes that is a DNA complexed with free hemin that also includes an iron-metal central ion. We found that the A $\beta$  1–40 peptide could also be oxidized by Dz-00. As the sequence modifications Dz-11 to Dz-18 did not alter the activity of Dz-00, we proposed to also apply the naturally occurring DNAzyme In1-sp. Based on its capability to form a G-quadruplex, we used this DNAzyme to oxidize the A $\beta$  peptide 1–40. The reaction velocity as a function of fluorescence was increased by 33.3% when catalyzed by In1-sp compared to free hemin. The yield as a fluorescence value was 4.6% higher compared to free hemin, providing a first hint toward the influence of DNAzymes in the progression of AD.

Consistent with these findings, HPSEC data indicate the DNAzyme-catalyzed formation of A $\beta$  1–40 dimers as well as agglomerates made of oxidized as well as non-oxidized A $\beta$  peptides. This leads to the thought that the oxidized form of A $\beta$  (covalently linked dimers) acts as agglomeration seeding in this process.<sup>29</sup> Due to the low yield of oxidized A $\beta$  formed by our DNAzymes, further in-depth investigation of the influence of oxidation on the A $\beta$  peptide structure by infrared spectroscopy and circular dichroism analysis did not show any significant change of the peptide structure at this point (Figure S8, Table S1).<sup>23,30</sup>

The role of A $\beta$  aggregation in AD development is still under debate,<sup>23,24,31,32</sup> but it has been shown that this aggregation could be a consequence of A $\beta$  oxidation. The concentrations of DNA and hemin as well as A $\beta$  1–40 applied in our study suggest an influence of DNAzymes in pathological states such as AD. Additionally, it was shown over the past years that G-quadruplexes are involved in human neurodegenerative diseases indicating their physiological relevance.<sup>33–36</sup> Because it was shown that intracellular G-quadruplexes exist,<sup>10,11,37</sup> the complex formation with hemin is possible as well as the oxidation of L-tyrosine and of the A $\beta$  1–40 peptide. Furthermore, it was shown by Rangan et al. in 2001 that even in vivo porphyrins can interact with G-quadruplex structures in human cells.<sup>38</sup> There are several sources in the cellular systems that produce, handle, and secrete peroxide species, such as H<sub>2</sub>O<sub>2</sub>,<sup>39</sup> giving an overall concentration in the blood or plasma of approximately 10  $\mu$ M.<sup>40</sup> Even the concentrations of free hemin up to the micromolar range have been reported, which can lead to A $\beta$  peptide accumulation accompanied by an increase of H<sub>2</sub>O<sub>2</sub> in these pathological states.<sup>13,39,41</sup> Also, the level of free DNA in blood circulation becomes elevated.<sup>42,43</sup> In brief, our experiments were inspired by these naturally occurring reaction conditions and concentrations and indeed display the contribution of DNAzymes in L-tyrosine oxidation and A $\beta$  1–40 oxidation and agglomeration. Furthermore, the catalytic activity of the DNAzymes tested in our studies was also retained in fetal bovine serum (FBS) as a model reaction medium being rather close to the above described physiological conditions (Figure S10).

## CONCLUSIONS

In the present paper, DNAzymes were employed as a catalyst to drive the oxidation of L-tyrosine toward dityrosine. This previously established reaction was employed as a model system to investigate the oxidation of A $\beta$  1–40 and its agglomeration that is linked to the development of AD. In here, we identified a stoichiometry of 1:10 between DNA and hemin to be most active, which also more likely reflects physiological conditions. To extend our studies on DNAzyme-driven A $\beta$  oxidation and agglomeration, we also applied a human genome-derived DNA sequence in DNAzyme formation to likewise catalyze the oxidation of A $\beta$ . Based on HPSEC and MALDI-TOF analysis, our data showed that this sequence could indeed form a more active DNAzyme compared to free hemin when catalyzing the oxidation of A $\beta$ . The fact that Dz-00, as an artificial DNAzyme, even showed an increase in velocity of 337.1% and in yield of 64.2% indicates that among the approximately 300,000 possible natural candidates in the human genome, there may be candidates for DNAzymes that exhibit a higher activity compared to In1-sp. These could also be involved in AD progression based on natural DNAzymes formed from DNA and hemin freely circulating in the blood system.<sup>9,11,12</sup>

## MATERIAL AND METHODS

**Materials.** Hemin(chloride), hydrogen peroxide (H<sub>2</sub>O<sub>2</sub>), sodium chloride, sodium phosphate, potassium phosphate, potassium hydroxide (KOH), dimethylsulfoxide (DMSO), L-tyrosine, tris(hydroxymethyl)aminomethane (TRIS), and ethylenediaminetetraacetic acid (EDTA) were purchased from Roth. All DNAs were purchased from biomers. The

FBS was purchased from Biochrom. The peptide A $\beta$  1–40 was purchased from AlexoTech. Dityrosine dihydrochloride was purchased from Cymit Quimica.

**Formation of Catalytically Active DNAzymes.** The ssDNA was dissolved in TE-buffer (10 mM TRIS, 1 mM EDTA) pH 7.3 and heated up to 85 °C for 5 min. After heating, it was cooled down gently by letting it stay for 30 min to correctly fold the G-quadruplex. A 5 mM hemin solution was prepared by dissolving hemin in DMSO. The solution was diluted with Milli-Q and added to the G-quadruplex solution in various stoichiometries that ended in final concentrations in the reactions of hemin as 100 nM (1:1), 200 nM (1:2), 500 nM (1:5), 1  $\mu$ M (1:10), and 2  $\mu$ M (1:20). The formation of DNAzymes was monitored spectroscopically by a change in absorption in the range of 380–420 nm using a plate reader (Tecan Infinite M200, Männerdorf Switzerland). The DNAzymes were used after at least 15 min formation time.

**Investigation of L-Tyrosine Oxidation.** DNA was used in a final concentration of 100 nM. Hemin concentration was adjusted in ratios ranging from 1:1 to 1:20 compared to DNA. H<sub>2</sub>O<sub>2</sub> was diluted in Milli-Q water to the appropriate concentrations and used in equimolar concentrations to L-tyrosine in the reactions. A stock solution of 200 mM L-tyrosine was prepared in 1 M KOH solution, diluted in Milli-Q water, and used in a final concentration of 250  $\mu$ M. The reactions were buffered with PBS (154 mM NaCl, 1.7 mM KH<sub>2</sub>PO<sub>4</sub>, 5 mM Na<sub>2</sub>HPO<sub>4</sub>) at pH 7.4. Reactions were followed by excitation of  $\lambda$  = 250 nm and emission of  $\lambda$  = 405 nm. The change of fluorescence at 405 nm was monitored using a plate reader (Tecan Infinite M200, Männerdorf Switzerland). We calibrated the system with dityrosine to calculate the activities of the DNAzymes (Figure S4).

**Investigation of A $\beta$  1–40 Oxidation.** The A $\beta$  1–40 peptide was dissolved in 15.6 mM KOH. H<sub>2</sub>O<sub>2</sub> was applied to the reactions in equimolar concentrations. DNAzymes were used in 100 nM concentration. The stoichiometry was chosen to be 1:10 to hemin. Hemin reaction was catalyzed by 1  $\mu$ M hemin. The samples were excited at  $\lambda$  = 250 nm and measured at an emission wavelength of  $\lambda$  = 405 nm using a plate reader.

**Size Exclusion Chromatography for Sample Analysis.** Samples of L-tyrosine or A $\beta$  peptide oxidation were analyzed by a HPLC-setup (Agilent) using a quaternary pump with a degasser and an autosampler from the 1100 series. Detectors used in this study were a diode array detector of the 1200 series for absorbance detection and a fluorescence detector of the 1100 series. PBS as an eluent was applied to a BioSep 5  $\mu$ M SEC-S2000 (Phenomenex) to separate the analytes. The measurements were recorded with OpenLab CDS Software and analyzed with Origin 2016.

## ■ ASSOCIATED CONTENT

### Supporting Information

The Supporting Information is available free of charge at <https://pubs.acs.org/doi/10.1021/acsomega.9b02645>.

CD-spectra of G-quadruplexes; kinetics behavior of DNAzyme formation: HPSEC chromatograms of L-tyrosine and dityrosine; calibration of dityrosine; mass spectra of L-tyrosine and dityrosine; DNAzyme stoichiometry; ATR–FTIR of A $\beta$  peptide; CD-spectra of A $\beta$  peptide; MALDI-TOF MAS analysis of A $\beta$  peptide; DNAzyme activity test in FBS; electron

paramagnetic resonance measurements of as-formed radicals; and proposed mechanism (PDF)

## ■ AUTHOR INFORMATION

### Corresponding Author

Julian Thiele – Leibniz-Institut für Polymerforschung Dresden e.V., 01069 Dresden, Germany; [orcid.org/0000-0001-5449-3048](https://orcid.org/0000-0001-5449-3048); Email: [thiele@ipfdd.de](mailto:thiele@ipfdd.de)

### Authors

Tony Köhler – Leibniz-Institut für Polymerforschung Dresden e.V., 01069 Dresden, Germany

Panagiotis A. Patsis – Leibniz-Institut für Polymerforschung Dresden e.V., 01069 Dresden, Germany; European Molecular Biology Laboratory, 69117 Heidelberg, Germany

Dominik Hahn – Leibniz-Institut für Polymerforschung Dresden e.V., 01069 Dresden, Germany; Center for Regenerative Therapies Dresden (CRTD), 01307 Dresden, Germany

André Ruland – Leibniz-Institut für Polymerforschung Dresden e.V., 01069 Dresden, Germany

Carolyn Naas – Leibniz-Institut für Polymerforschung Dresden e.V., 01069 Dresden, Germany

Martin Müller – Leibniz-Institut für Polymerforschung Dresden e.V., 01069 Dresden, Germany; [orcid.org/0000-0001-8961-4604](https://orcid.org/0000-0001-8961-4604)

Complete contact information is available at: <https://pubs.acs.org/10.1021/acsomega.9b02645>

### Author Contributions

All authors have given approval to the final version of the manuscript.

### Funding

The authors thank the Federal Ministry of Education and Research (BMBF, Biotechnology2020+: Leibniz Research Cluster, 031A360C) and the German Research Foundation (DFG, TH 2037/1-1 and Research Training Group GRK 1865: Hydrogel-based Microsystems) for financial support. J.T. acknowledges the Young Investigator Program of the Technische Universität Dresden.

### Notes

The authors declare no competing financial interest.

## ■ ACKNOWLEDGMENTS

We thank Birgit Urban for measuring CD and ATR–FTIR spectra. We also thank Dr. Sandra Höfgen (HKI Jena) and Dr. Anika Kaufman (IPF Dresden) for fruitful discussions during preparation of this manuscript.

## ■ REFERENCES

- (1) Rhodes, D.; Lipps, H. J. G-quadruplexes and their regulatory roles in biology. *Nucleic Acids Res.* **2015**, *43*, 8627–8637.
- (2) Gerasimov, J. Y.; Schaefer, C. S.; Yang, W.; Grout, R. L.; Lai, R. Y. Development of an electrochemical insulin sensor based on the insulin-linked polymorphic region. *Biosens. Bioelectron.* **2013**, *42*, 62–68.
- (3) Huang, Y.; Xu, W.; Liu, G.; Tian, L. A pure DNA hydrogel with stable catalytic ability produced by one-step rolling circle amplification. *Chem. Commun.* **2017**, *53*, 3038–3041.
- (4) Kahn, J. S.; Hu, Y.; Willner, I. Stimuli-Responsive DNA-Based Hydrogels: From Basic Principles to Applications. *Acc. Chem. Res.* **2017**, *50*, 680–690.
- (5) Li, W.; Li, Y.; Liu, Z.; Lin, B.; Yi, H.; Xu, F.; Nie, Z.; Yao, S. Insight into G-quadruplex-hemin DNAzyme/RNAzyme: adjacent

adenine as the intramolecular species for remarkable enhancement of enzymatic activity. *Nucleic Acids Res.* **2016**, *44*, 7373–7384.

(6) Liu, B.; Shang, H.; Li, D. General peroxidase activity of a parallel G-quadruplex-hemin DNAzyme formed by Pu39WT - a mixed G-quadruplex forming sequence in the Bcl-2 P1 promoter. *Chem. Cent. J.* **2014**, *8*, 43.

(7) Travascio, P.; Li, Y.; Sen, D. DNA-enhanced peroxidase activity of a DNA aptamer-hemin complex. *Chem. Biol.* **1998**, *5*, 505–517.

(8) Breaker, R. R.; Joyce, G. F. A DNA enzyme that cleaves RNA. *Chem. Biol.* **1994**, *1*, 223–229.

(9) Todd, A. K.; Johnston, M.; Neidle, S. Highly prevalent putative quadruplex sequence motifs in human DNA. *Nucleic Acids Res.* **2005**, *33*, 2901–2907.

(10) Henderson, A.; Wu, Y.; Huang, Y. C.; Chavez, E. A.; Platt, J.; Johnson, F. B.; Brosh, R. M., Jr.; Sen, D.; Lansdorp, P. M. Detection of G-quadruplex DNA in mammalian cells. *Nucleic Acids Res.* **2014**, *42*, 860–869.

(11) Hänsel-Hertsch, R.; Di Antonio, M.; Balasubramanian, S. DNA G-quadruplexes in the human genome: detection, functions and therapeutic potential. *Nat. Rev. Mol. Cell Biol.* **2017**, *18*, 279–284.

(12) Huppert, J. L.; Balasubramanian, S. Prevalence of quadruplexes in the human genome. *Nucleic Acids Res.* **2005**, *33*, 2908–2916.

(13) Al-Hilaly, Y. K.; Williams, T. L.; Stewart-Parker, M.; Ford, L.; Skaria, E.; Cole, M.; Bucher, W.; Morris, K. L.; Sada, A.; Thorpe, J. R.; Serpell, L. C. A central role for dityrosine crosslinking of Amyloid- $\beta$  in Alzheimer's disease. *Acta Neuropathol. Commun.* **2013**, *1*, 83.

(14) Bush, A. I. The metallobiology of Alzheimer's disease. *Trends Neurosci.* **2003**, *26*, 207–214.

(15) Chiziane, E.; Telemann, H.; Krueger, M.; Adler, J.; Arnhold, J.; Alia, A.; Flemmig, J. Free Heme and Amyloid- $\beta$ : A Fatal Liaison in Alzheimer's Disease. *J. Alzheim. Dis.* **2018**, *61*, 963–984.

(16) Gross, A. J.; Sizer, I. W. The Oxidation of Tyramine, Tyrosine and Related Compounds by Peroxidase. *J. Biol. Chem.* **1959**, *234*, 1611.

(17) Einarson, O. J.; Sen, D. Self-biotinylation of DNA G-quadruplexes via intrinsic peroxidase activity. *Nucleic Acids Res.* **2017**, *45*, 9813–9822.

(18) Nakayama, S.; Sintim, H. O. Biomolecule detection with peroxidase-mimicking DNAszymes; expanding detection modality with fluorogenic compounds. *Mol. Biosyst.* **2010**, *6*, 95–97.

(19) Nakayama, S.; Sintim, H. O. Investigating the interactions between cations, peroxidation substrates and G-quadruplex topology in DNAzyme peroxidation reactions using statistical testing. *Anal. Chim. Acta* **2012**, *747*, 1–6.

(20) Nakayama, S.; Wang, J.; Sintim, H. O. DNA-based peroxidation catalyst-what is the exact role of topology on catalysis and is there a special binding site for catalysis? *Chemistry* **2011**, *17*, 5691–5698.

(21) Rojas, A. M.; Gonzalez, P. A.; Antipov, E.; Klivanov, A. M. Specificity of a DNA-based (DNAzyme) peroxidative biocatalyst. *Biotechnol. Lett.* **2007**, *29*, 227–232.

(22) Flemmig, J.; Zámocký, M.; Alia, A. Amyloid  $\beta$  and free heme: bloody new insights into the pathogenesis of Alzheimer's disease. *Neural Regen. Res.* **2018**, *13*, 1170–1174.

(23) Klementieva, O.; Willen, K.; Martinsson, I.; Israelsson, B.; Engdahl, A.; Cladera, J.; Uvdal, P.; Gouras, G. K. Pre-plaque conformational changes in Alzheimer's disease-linked A $\beta$  and APP. *Nat. Commun.* **2017**, *8*, 14726.

(24) Khodarahmi, R.; Ashrafi-Kooshk, M. R. Is there correlation between A $\beta$ -heme peroxidase activity and the peptide aggregation state? A literature review combined with hypothesis. *Int. J. Biol. Macromol.* **2017**, *100*, 18–36.

(25) Xiao, Y.; Pavlov, V.; Niazov, T.; Dishon, A.; Kotler, M.; Willner, I. Catalytic Beacons for the Detection of DNA and Telomerase Activity. *J. Am. Chem. Soc.* **2004**, *126*, 7430–7431.

(26) Jayakumar, R.; Kusiak, J. W.; Chrest, F. J.; Demehin, A. A.; Murali, J.; Wersto, R. P.; Nagababu, E.; Ravi, L.; Rifkind, J. M. Red cell perturbations by amyloid  $\beta$ -protein. *Biochim. Biophys. Acta Gen. Subj.* **2003**, *1622*, 20–28.

(27) Atamna, H. Heme binding to Amyloid- $\beta$  peptide: Mechanistic role in Alzheimer's disease. *J. Alzheimer's Dis.* **2006**, *10*, 255–266.

(28) Atamna, H.; Boyle, K. Amyloid-beta peptide binds with heme to form a peroxidase: relationship to the cytopathologies of Alzheimer's disease. *Proc. Natl. Acad. Sci. U.S.A.* **2006**, *103*, 3381–3386.

(29) Galante, D.; Corsaro, A.; Florio, T.; Vella, S.; Pagano, A.; Sbrana, F.; Vassalli, M.; Perico, A.; D'Arrigo, C. Differential toxicity, conformation and morphology of typical initial aggregation states of A $\beta$ 1-42 and A $\beta$ py3-42 beta-amyloids. *Int. J. Biochem. Cell Biol.* **2012**, *44*, 2085–2093.

(30) Kok, W. M.; Scanlon, D. B.; Karas, J. A.; Miles, L. A.; Tew, D. J.; Parker, M. W.; Barnham, K. J.; Hutton, C. A. Solid-phase synthesis of homodimeric peptides: preparation of covalently-linked dimers of amyloid  $\beta$  peptide. *Chem. Commun.* **2009**, 6228–6230.

(31) Kok, W. M.; Cottam, J. M.; Ciccotosto, G. D.; Miles, L. A.; Karas, J. A.; Scanlon, D. B.; Roberts, B. R.; Parker, M. W.; Cappai, R.; Barnham, K. J.; Hutton, C. A. Synthetic dityrosine-linked  $\beta$ -amyloid dimers form stable, soluble, neurotoxic oligomers. *Chem. Sci.* **2013**, *4*, 4449.

(32) Ke, Z.; Huang, Q. Effect of protein structure and/or conformation on the dityrosine cross-linking induced by haem-hydrogen peroxide. *Biochim. Biophys. Acta* **2016**, *1860*, 2232–2238.

(33) Geng, Y.; Liu, C.; Zhou, B.; Cai, Q.; Miao, H.; Shi, X.; Xu, N.; You, Y.; Fung, C. P.; Din, R. U.; Zhu, G. The crystal structure of an antiparallel chair-type G-quadruplex formed by Bromo-substituted human telomeric DNA. *Nucleic Acids Res.* **2019**, *47*, 5395–5404.

(34) Liu, C.; Geng, Y.; Miao, H.; Shi, X.; You, Y.; Xu, N.; Zhou, B.; Zhu, G. G-quadruplex structures formed by human telomeric DNA and C9orf72 hexanucleotide repeats. *Biophys. Rev.* **2019**, *11*, 389–393.

(35) Simone, R.; Fratta, P.; Neidle, S.; Parkinson, G. N.; Isaacs, A. M. G-quadruplexes: Emerging roles in neurodegenerative diseases and the non-coding transcriptome. *FEBS Lett.* **2015**, *589*, 1653–1668.

(36) Wu, Y.; Brosh, R. M., Jr. G-quadruplex nucleic acids and human disease. *FEBS J.* **2010**, *277*, 3470–3488.

(37) Biffi, G.; Tannahill, D.; McCafferty, J.; Balasubramanian, S. Quantitative visualization of DNA G-quadruplex structures in human cells. *Nat. Chem.* **2013**, *5*, 182–186.

(38) Rangan, A.; Fedoroff, O. Y.; Hurley, L. H. Induction of duplex to G-quadruplex transition in the c-myc promoter region by a small molecule. *J. Biol. Chem.* **2001**, *276*, 4640–4646.

(39) Chance, B.; Sies, H.; Boveris, A. Hydroperoxide Metabolism in Mammalian Organs. *Physiol. Rev.* **1979**, *59*, 527–605.

(40) Forman, H. J.; Bernardo, A.; Davies, K. J. A. What is the concentration of hydrogen peroxide in blood and plasma? *Arch. Biochem. Biophys.* **2016**, *603*, 48–53.

(41) Thiabaud, G.; Pizzocaro, S.; Garcia-Serres, R.; Latour, J.-M.; Monzani, E.; Casella, L. Heme Binding Induces Dimerization and Nitration of Truncated  $\beta$ -Amyloid Peptide A $\beta$ 16 Under Oxidative Stress. *Angew. Chem., Int. Ed.* **2013**, *52*, 8041–8044.

(42) Swarup, V.; Rajeswari, M. R. Circulating (cell-free) nucleic acids - A promising, non-invasive tool for early detection of several human diseases. *FEBS Lett.* **2007**, *581*, 795–799.

(43) Meddeb, R.; Dache, Z. A. A.; Thezenas, S.; Otandault, A.; Tanos, R.; Pastor, B.; Sanchez, C.; Azzi, J.; Tusch, G.; Azan, S.; Mollevi, C.; Adenis, A.; El Messaoudi, S.; Blache, P.; Thierry, A. R. Quantifying circulating cell-free DNA in humans. *Sci. Rep.* **2019**, *9*, 5220.